Supplemental Material for "Shortcuts to Adiabaticity for the Quantum Rabi Model: Efficient Generation of Giant Entangled Cat States via Parametric Amplification"

Ye-Hong Chen,[1] Wei Qin,[1] Xin Wang,[1,2] Adam Miranowicz,[1,3] and Franco Nori[1,4]

[1] *Theoretical Quantum Physics Laboratory, RIKEN Cluster for Pioneering Research, Wako-shi, Saitama 351-0198, Japan*
[2] *Institute of Quantum Optics and Quantum Information, School of Science, Xi'an Jiaotong University, Xi'an 710049, China*
[3] *Faculty of Physics, Adam Mickiewicz University, 61-614 Poznań, Poland*
[4] *Department of Physics, University of Michigan, Ann Arbor, Michigan 48109-1040, USA*

(Dated: December 26, 2020)

In this Supplemental Material, we first discuss the influence of the nonadiabatic transition caused by mapping the system dynamics into the time-dependent squeezed-light frame. Using the transitionless algorithm, we show how to counteract such a nonadiabatic transition with an additional drive, so as to design a shortcuts-to-adiabatic passage to rapidly generate giant entangled cat states. Then, we show how to minimize the influence of the squeezing-induced fluctuation noise by coupling the cavity to a squeezed-vacuum reservoir. Thirdly, we present a possible problem in turning off the parametric drive when the target state is generated in the squeezed-light frame via the adiabatic process.

The parameters and operators in this supplemental material are defined to be the same as those of the main text.

S1. EFFECTIVE HAMILTONIAN AND DISSIPATION DYNAMICS OF THE SYSTEM

A. Counteracting the nonadiabatic transition caused by the time-dependent unitary transformation

We begin with a largely detuned Jaynes-Cummings (JC) Hamiltonian driven by a time-dependent parametric (two-photon) drive $\Omega_r(t)$,

$$H_1(t)=\Delta a^\dagger a-\left[\frac{\Omega_r(t)}{2}a^2-\lambda a^\dagger\sigma+\text{h.c.}\right]. \tag{S1}$$

In the time-dependent squeezed-light frame determined by the squeezing operator $S(t)=\exp\left[r(t)(a^{\dagger 2}-a^2)/2\right]$, with a real squeezing parameter $r(t)$ satisfying $\tanh\left[2r(t)\right]=\Omega_r(t)/\Delta$, the Hamiltonian of the system is composed of the following terms:

$$\begin{aligned}
H_{\text{S1}}(t)&=S^\dagger(t)H_1(t)S(t)-iS^\dagger(t)\dot{S}(t)\\
&=H_{\text{S}-\text{Rabi}}(t)+H_{\text{err}}(t)+H_{\text{NA}}(t),\\
H_{\text{S}-\text{Rabi}}(t)&=\Delta\text{sech}[2r(t)]a^\dagger a+\lambda\exp\left[r(t)\right]\sigma_x(a^\dagger+a)/2,\\
H_{\text{err}}(t)&=-i\lambda\exp\left[-r(t)\right]\sigma_y(a^\dagger-a)/2,\\
H_{\text{NA}}(t)&=-i\dot{r}(t)(a^{\dagger 2}-a^2)/2.
\end{aligned} \tag{S2}$$

The Hamiltonian $H_{\text{S}-\text{Rabi}}$ describes the $\sigma_x X$ Rabi interaction in the squeezed-light frame, where $X=(a+a^\dagger)/2$ is the canonical position operator. The Hamiltonian $H_{\text{err}}(t)$ describes the $\sigma_y Y$ interaction, where $Y=i(a^\dagger-a)/2$ is the canonical momentum operator, and can be considered an error term, which can be neglected when $\lambda\ll\Delta$ and $\lambda/\Delta\ll r(t)$. When $r(t)\sim\lambda/\Delta$, the error term $H_{\text{err}}(t)$ can be neglected by applying a strong drive $\Omega\sigma_x$ ($\Omega\gtrsim\Delta$), which induces the coupling of $H_{\text{err}}(t)$ with a large detuning in the σ_y-direction.

The last term in $H_{\text{S1}}(t)$, i.e., $H_{\text{NA}}(t)=-iS^\dagger(t)\dot{S}(t)$, describes a nonadiabatic transition induced by mapping the system dynamics into the time-dependent squeezed-light frame. It describes the population transfer between different basis in the squeezed-light frame. According to Berry's transitionless algorithm, we can add a term

$$H_{\text{SA}}(t)=iS^\dagger(t)\dot{S}(t)=i\dot{r}(t)(a^{\dagger 2}-a^2)/2, \tag{S3}$$

into the Hamiltonian $H_{\text{S1}}(t)$ to counteract the nonadiabatic transition. Then, in the laboratory frame, the additional Hamiltonian H_{SA} reads

$$H_{\text{add}}(t)=S(t)H_{\text{SA}}(t)S^\dagger=i\dot{r}(t)(a^{\dagger 2}-a^2)/2. \tag{S4}$$

This implies that the cavity mode is subject to another two-photon drive, which has an amplitude $\Omega_i(t) = \dot{r}(t)$, a frequency ω_p, and is $\pi/2$-dephased from $\Omega_r(t)$. By adding this additional Hamiltonian $H_{\rm add}(t)$ into the Hamiltonian $H_1(t)$, we obtain the Hamiltonian $H_0(t)$ required for the STA protocol, i.e., the Hamiltonian of Eq. (6) of the main text:

$$H_0(t) = \Delta a^\dagger a + \Omega\sigma_x - \left[\frac{\Omega_r(t) + i\Omega_i(t)}{2}a^2 - \lambda a^\dagger\sigma + \text{h.c.}\right]. \tag{S5}$$

Then, we are allowed to rapidly change the squeezing parameter $r(t)$, such that we can quickly adjust the effective qubit-cavity coupling $\lambda\exp[r(t)]/2$ in the squeezed-light frame.

This is very important, because applying the STA protocol requires to rapidly change the control parameter, i.e., the normalized coupling strength.

B. STA process with parametric drivings

To construct the STA passage, we divide the Hamiltonian $H_S(t)$ into two parts:

$$H_S(t) = H_{\rm ref}(t) + H_{\rm aux}(t). \tag{S6}$$

Here, the Hamiltonian

$$H_{\rm ref}(t) = \Delta\text{sech}[2r(t)]a^\dagger a + \sigma_x[\chi(t)a^\dagger + \chi^*(t)a], \tag{S7}$$

is considered as the reference Hamiltonian [with an undetermined parameter $\chi(t)$] for constructing shortcuts,

$$H_{\rm aux}(t) = \frac{\lambda e^{r(t)}}{2}\sigma_x(a^\dagger + a) - \sigma_x[\chi(t)a^\dagger + \chi^*(t)a], \tag{S8}$$

is an auxiliary Hamiltonian. The reference Hamiltonian $H_{\rm ref}(t)$ takes the same form as the Rabi Hamiltonian $H_R(t)$ [Eq. (1) of the main text], i.e., $H_{\rm ref}(t) :\Rightarrow H_R(t)$, by setting:

$$\omega_q \ll \omega_c, \quad \omega_c :\Rightarrow \Delta\text{sech}[2r(t)], \quad g :\Rightarrow \chi(t). \tag{S9}$$

Then, when we choose the parameters to satisfy

$$\eta(t) = \frac{g}{\omega_c} = \frac{\chi(t)}{\Delta\text{sech}[2r(t)]}, \quad \dot{\eta}(t) = \frac{i}{2}\left[\lambda e^{r(t)} - 2\chi(t)\right], \tag{S10}$$

$H_{\rm aux}(t)$ is exactly the CD driving Hamiltonian for the reference Hamiltonian $H_{\rm ref}(t)$, i.e., $H_{\rm aux}(t) :\Rightarrow H_{\rm CD}(t)$. Hence, according to the transitionless algorithm, the CD driving Hamiltonian $H_{\rm aux}(t)$ can actually drive the system to evolve along an eigenstate of $H_{\rm ref}(t)$. The evolution path for our STA protocol is then given as (in the squeezed-light frame)

$$|E_0(t)\rangle_S = \frac{1}{\sqrt{2}}\left[|+_x\rangle|-\eta(t)\rangle + |-_x\rangle|\eta(t)\rangle\right], \tag{S11}$$

where $|\pm_x\rangle$ are the eigenstates of the Pauli matrix σ_x. In the lab frame, the STA evolution path is $S[r(t)]|E_0(t)\rangle_S$. After some algebra, we can counteract the undetermined parameter $\chi(t)$ and obtain the equations of motion for the coherent state amplitude $\eta(t)$:

$$\begin{aligned}\text{Re}[\dot{\eta}(t)] =& \Delta\text{Im}[\eta(t)]\text{sech}2r(t),\\ \text{Im}[\dot{\eta}(t)] =& \frac{\lambda}{2}\exp[r(t)] - \Delta\text{Re}[\eta(t)]\text{sech}2r(t).\end{aligned} \tag{S12}$$

Thus, Eq. (9) of the main text is obtained. The final state in the laboratory frame is

$$S(t_f)|E_0(t_f)\rangle_S = \frac{1}{\sqrt{2}}\left(|+_x\rangle|-\eta(t_f)\rangle + |-_x\rangle|\eta(t_f)\rangle\right), \tag{S13}$$

which is an entangled cat state. Here, $S(t_f) = 1$ is given according to $r(t_f) = 0$.

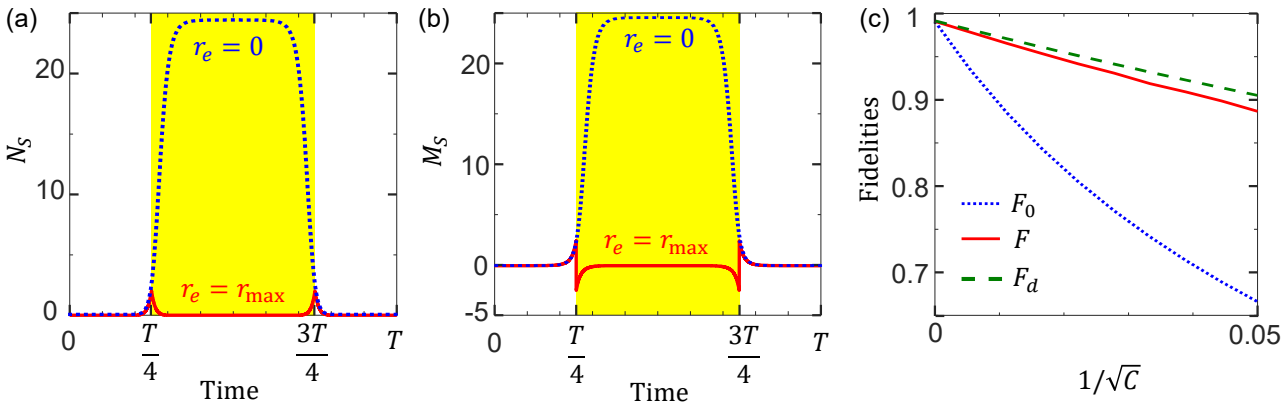

FIG. S1: Parameters (a) N_S and (b) M_S characterizing the squeezing-induced noise for $r_{\max} = 2.3$ and $\Omega = 0$. Blue-dotted curve in (a) [(b)]: Parameter N_S (M_S) without coupling the cavity to the squeezed-vacuum reservoir (i.e., $r_e = 0$); Red-solid curve in (a) [(b)]: Parameter N_S (M_S) when the system is coupled to the squeezed-vacuum reservoir during $T/4 \lesssim t \lesssim 3T/4$ [i.e., r_e is given according to Eq. (S21)]. The yellow-shaded area in (a) or (b) denotes when the cavity is coupled to the squeezed-vacuum reservoir. (c) Fidelities of the ground state $|G\rangle$ versus $1/\sqrt{C}$ calculated by: (blue-dotted curve representing F_0) the noise-included master equation in Eq. (S16) when $r_e = 0$; (red-solid curve representing F) the noise-included master equation when coupling the cavity to the squeezed-vacuum; (green-dashed curve representing F_d) the effective master equation in Eq. (S23). The parameter $C = \lambda^2/\kappa\gamma$ is the cooperativity, and we assume the dissipation rates $\gamma = \kappa$ for simplicity.

C. Minimizing the influence of the squeezing-induced fluctuation noise

The Markovian master equation, for a cavity interacting with a broadband squeezed-vacuum reservoir (at zero temperature with squeezing parameter r_e and reference phase φ_e), has been well studied (see, e.g., Ref. [S1]). For our STA protocol, when the cavity couples to the squeezed-vacuum reservoir, the master equation in the laboratory frame is

$$\begin{aligned}\dot{\rho}(t) =& i[\rho(t), H_0(t)] + \frac{1}{2}\left[2L_\gamma\rho(t)L_\gamma^\dagger - L_\gamma^\dagger L_\gamma\rho(t) - \rho(t)L_\gamma^\dagger L_\gamma\right] \\ &+ \frac{1}{2}(N+1)\left[2L_\kappa\rho(t)L_\kappa^\dagger - L_\kappa^\dagger L_\kappa\rho(t) - \rho(t)L_\kappa^\dagger L_\kappa\right] \\ &+ \frac{1}{2}N\left[2L_\kappa^\dagger\rho(t)L_\kappa - L_\kappa L_\kappa^\dagger\rho(t) - \rho(t)L_\kappa L_\kappa^\dagger\right] \\ &- \frac{1}{2}M\left[2L_\kappa^\dagger\rho(t)L_\kappa^\dagger - L_\kappa^\dagger L_\kappa^\dagger\rho(t) - \rho(t)L_\kappa^\dagger L_\kappa^\dagger\right] \\ &- \frac{1}{2}M^*\left[2L_\kappa\rho(t)L_\kappa - L_\kappa L_\kappa\rho(t) - \rho(t)L_\kappa L_\kappa\right]. \end{aligned} \tag{S14}$$

Here, $L_\gamma = \sqrt{\gamma}\sigma$ and $L_\kappa = \sqrt{\kappa}a$ describe the qubit and cavity decays, with decay rates γ and κ, respectively. The parameters

$$N = \sinh^2(r_e), \quad \text{and} \quad M = \cosh(r_e)\sinh(r_e)\exp(-i\varphi_e), \tag{S15}$$

describe thermal noise and two-photon correlation noise caused by the squeezed-vacuum reservoir, respectively.

By mapping the system dynamics into the time-dependent squeezed-light frame with $S(t)$, the master equation becomes

$$\begin{aligned}\dot{\rho}_S(t) =& i[\rho_S(t), H_{\text{S-Rabi}}(t) + H_{\text{err}}(t)] + \frac{1}{2}\left[2L_\gamma\rho_S(t)L_\gamma^\dagger - L_\gamma^\dagger L_\gamma\rho_S(t) - \rho_S(t)L_\gamma^\dagger L_\gamma\right] \\ &+ \frac{1}{2}(N_S+1)\left[2L_\kappa\rho_S(t)L_\kappa^\dagger - L_\kappa^\dagger L_\kappa\rho_S(t) - \rho_S(t)L_\kappa^\dagger L_\kappa\right] \\ &+ \frac{1}{2}N_S\left[2L_\kappa^\dagger\rho_S(t)L_\kappa - L_\kappa L_\kappa^\dagger\rho_S(t) - \rho_S(t)L_\kappa L_\kappa^\dagger\right] \\ &- \frac{1}{2}M_S\left[2L_\kappa^\dagger\rho_S(t)L_\kappa^\dagger - L_\kappa^\dagger L_\kappa^\dagger\rho_S(t) - \rho_S(t)L_\kappa^\dagger L_\kappa^\dagger\right] \\ &- \frac{1}{2}M_S^*\left[2L_\kappa\rho_S(t)L_\kappa - L_\kappa L_\kappa\rho_S(t) - \rho_S(t)L_\kappa L_\kappa\right], \end{aligned} \tag{S16}$$

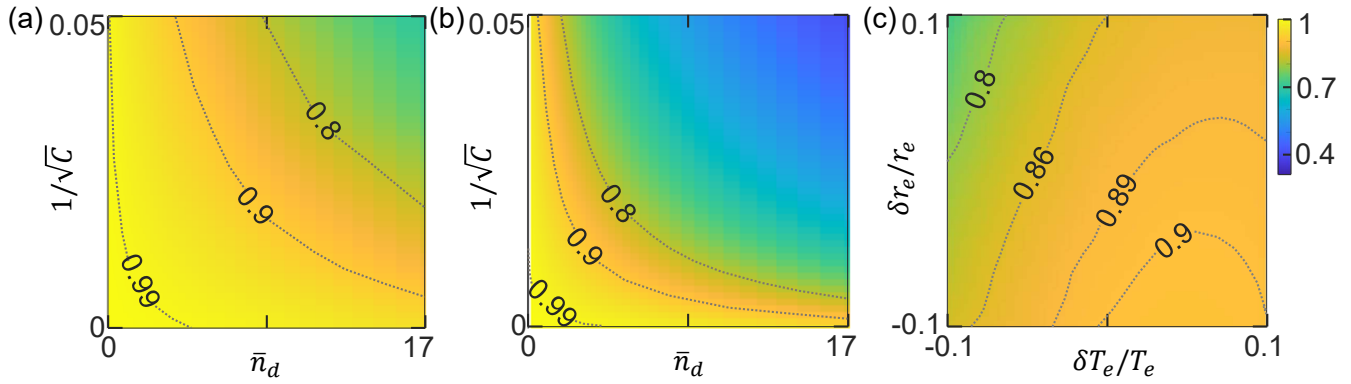

FIG. S2: blue Fidelities F of the entangled cat state for the STA protocol with $T = 20/\Delta$ and $\lambda = 0.045\Delta$: (a) [(b)] Fidelity F versus the cooperativity C and the predicted mean photon number $\bar{n}_d = |\eta|^2$, when the cavity is coupled (decoupled) to the squeezed-vacuum reservoir. For the panels (a) and (b), we choose the squeezing parameter $r_{\max} \in [0, 3]$ corresponding to the $\bar{n}_d = |\eta|^2 \in [0, 17]$. (c) Fidelity F versus imperfections of the parameters r_e and T_e. For the panel (c), the squeezing parameter is $r_{\max} = 2.3$.

where $\rho_S(t) = S^\dagger(t)\rho(t)S(t)$ is the density operator of the system in the squeezed-light frame, and

$$\begin{aligned} N_S =& \cosh^2[r(t)]\sinh^2(r_e) + \sinh^2[r(t)]\cosh^2(r_e) + \frac{1}{2}\sinh[2r(t)]\sinh(2r_e)\cos(\varphi_e), \\ M_S =& \{\sinh[r(t)]\cosh(r_e) + \exp(-i\varphi_e)\cosh[r(t)]\sinh(r_e)\} \\ & \times \{\cosh[r(t)]\cosh(r_e) + \exp(i\varphi_e)\sinh[r(t)]\sinh(r_e)\}, \end{aligned} \tag{S17}$$

characterize additional noises of the system in the squeezed-light frame. When $r_e = 0$, N_S and M_S characterize the squeezing-induced noise. For simplicity, we can assume $\varphi_e = \pi$, and obtain

$$N_S = \sinh^2[r_S(t)], \quad \text{and} \quad M_S = \cosh[r_S(t)]\sinh[r_S(t)], \tag{S18}$$

where $r_S(t) = r(t) - r_e$. Then, to minimize the parameters $|N_S|$ and $|M_S|$, we need to minimize the parameter $|r_S(t)|$.

The waveform of $r(t)$ of the STA protocol is approximately a square wave when

$$r(t) = \frac{r_{\max}}{1 + \exp[f_0 \cos(2\pi t/T)]}, \tag{S19}$$

where $f_0 = 10$ controls the initial and final values of the squeezing parameter $r(t)$. Substituting Eq. (S19) into Eq. (S18) and assuming $r_e = 0$, in Figs. S1(a) and S1(b), we show the parameters N_S and M_S describing the squeezing-induced noise (see the blue-dotted curves). As shown, the squeezing-induced noise affects the system dynamics especially when $r(t)$ reaches its maximum value $r_{\max}$, i.e., $r(t) \approx r_{\max}$. We accordingly calculate the fidelity $F_0 = |\langle G|\rho_S(t_f)|G\rangle|$ to show the influence of the squeezing-induced noise [see the blue-dotted curve in Fig. S1(c)]. Here, $|G\rangle$ is the ground state of the Rabi model in the DSC regime [see Eq. (2) of the main text]. The fidelity F_0 decreases very fast when the dissipation increases.

To minimize the parameter $|r_S(t)|$, according to the properties of $\cos(2\pi t/T)$, we can choose

$$r_e = \begin{cases} 0, & (0 \lesssim t \lesssim T/4) \\ r_{\max}, & (T/4 \lesssim t \lesssim 3T/4) \\ 0, & (3T/4 \lesssim t \lesssim T) \end{cases} \tag{S20}$$

i.e., the total interaction time between the cavity and the squeezed-vacuum reservoir is $T_e = T/2$, resulting in

$$r_S(t) = \begin{cases} \dfrac{r_{\max}}{1 + \exp[f_0 \cos(2\pi t/T)]}, & (0 \lesssim t \lesssim T/4) \\ \dfrac{-r_{\max}}{1 + \exp[-f_0 \cos(2\pi t/T)]}, & (T/4 \lesssim t \lesssim 3T/4) \\ \dfrac{r_{\max}}{1 + \exp[f_0 \cos(2\pi t/T)]}. & (3T/4 \lesssim t \lesssim T) \end{cases} \tag{S21}$$

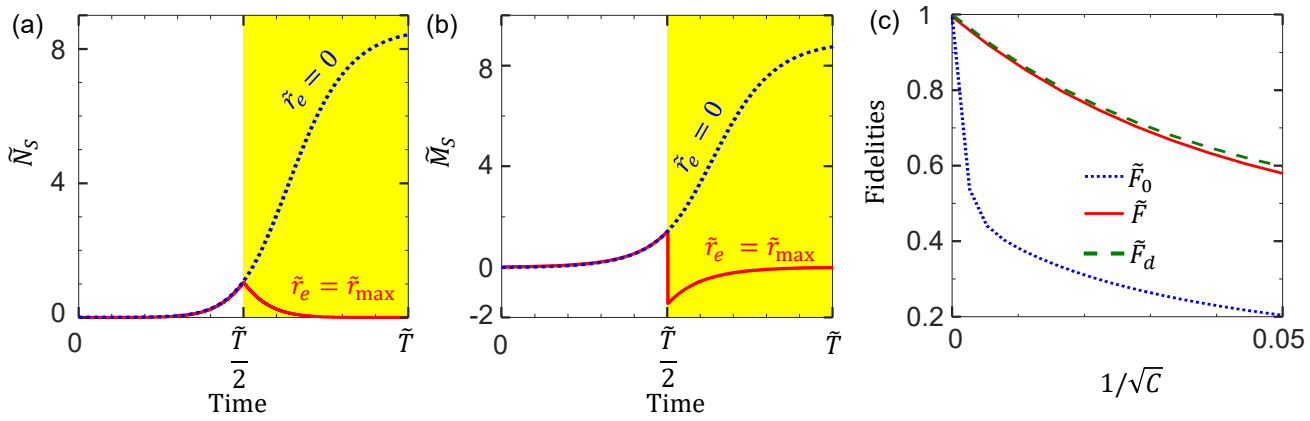

FIG. S3: Parameters (a) $\tilde{N}_S$ and (b) $\tilde{M}_S$ characterizing the squeezing-induced noise for $\tilde{r}_{\max} = 1.8$. Blue-dotted curve in (a) [(b)]: parameter $\tilde{N}_S$ ($\tilde{M}_S$) without coupling the cavity to the squeezed-vacuum reservoir (i.e., $\tilde{r}_e = 0$); Red-solid curve in (a) [(b)]: parameter $\tilde{N}_S$ ($\tilde{M}_S$) when the system is coupled to the squeezed-vacuum reservoir during $\tilde{T}/2 \lesssim t \lesssim \tilde{T}$ [i.e., $\tilde{r}_e$ is given according to Eq. (S25)]. The yellow-shaded area in (a) or (b) denotes that the cavity is coupled to the squeezed-vacuum reservoir. (c) Fidelities of the squeezed ground state $|SG\rangle = S(t_f)|G\rangle$ versus $1/\sqrt{C}$ calculated by: (blue-dotted curve representing $\tilde{F}_0$) the noise-included master equation in Eq. (S16) when $r_e = 0$; (red-solid curve representing $\tilde{F}$) the noise-included master equation when coupling the cavity to the squeezed-vacuum reservoir; (green-dashed curve representing $\tilde{F}_d$) the effective master equation in Eq. (S23).

Then, substituting Eq. (S21) into Eq. (S18), we plot the parameters N_S and M_S [see the red-solid curves in Fig. S1(a) and S1(b)]. We can accordingly calculate the average values

$$A_{N_S} = \frac{1}{T}\int_0^{t_f} |N_S| dt \approx 0.08, \quad \text{and} \quad A_{M_S} = \frac{1}{T}\int_0^{t_f} |M_S| dt \approx 0.14, \tag{S22}$$

which means that the additional noises in Eq. (S16) weakly affect the system dynamics. Thus, the fidelity of the target state $|G\rangle$ is significantly improved [see the red-solid curve in Fig. S1(c)], e.g., from $\sim 65\%$ to $\sim 89\%$ when $1/\sqrt{C} = 0.05$. When the desired mean photon number $\bar{n}_d$ of the target state increases, the influence of the cavity loss increases [see Figs. S3(a) and S3(b)]. These figures show the fidelities of the target state when the cavity is coupled and decoupled to the squeezed-vacuum reservoir, respectively. According to the comparison between Figs. S1(a) and S1(b), coupling the cavity to the squeezed-vacuum reservoir can effectively suppress the influence of the cavity loss. Thus, the giant ($\bar{n}_d \gtrsim 10$) entangled cat states can be generated with a high fidelity. By defining the imperfection of a parameter $*$ as $\delta* = *' - *$, the influence of the imperfections of the parameters T_e and r_e is shown in Fig. S1(c). This figure shows that, slightly decreasing the squeezing parameter r_e or increasing the interaction time T_e can improve the fidelity F. Note that a 10% imperfection of the parameter r_e only causes a 3% change in the fidelity, thus the STA protocol is mostly insensitive to the imperfections of the parameter r_e. When the interaction time T_e between the cavity and the squeezed-vacuum reservoir is long enough, our STA protocol is mostly insensitive to the imperfections of the parameter T_e.

When coupling the cavity to the squeezed-vacuum reservoir during $T/4 \lesssim t \lesssim 3T/4$, the evolution can be approximately described by the standard Lindblad master equation

$$\dot{\rho_S}(t) \approx i[\rho_S(t), H_{\text{S-Rabi}}(t)] + \frac{1}{2}\sum_{m=\kappa,\gamma}\left[2L_m\rho_S(t)L_m^\dagger - L_m^\dagger L_m\rho_S(t) - \rho_S(t)L_m^\dagger L_m\right], \tag{S23}$$

which is Eq. (10) of the main text. As shown in Fig. S1(c), the Lindblad master equation can well describe the dynamics when the cavity is coupled to the squeezed-vacuum reservoir.

This strategy is also applicable in the adiabatic protocol to minimize the influence of the squeezing-induced noise. For the adiabatic protocol, the squeezing parameter $\tilde{r}(t)$ is

$$\tilde{r}(t) = \frac{\tilde{r}_{\max}}{1 + \exp\left[\tilde{f}_0(1/2 - t/\tilde{T})\right]}, \tag{S24}$$

where $\tilde{f}_0 = 10$ controls the initial and final values of $\tilde{r}(t)$. Substituting Eq. (S24) into Eq. (S17) and assuming $\tilde{r}_e = 0$, we plot the parameters $\tilde{N}_S$ and $\tilde{M}_S$ in Figs. S3(a) and S3(b). We denote $\tilde{*}$ ($* = r,\ T,\ \ldots$) to represent the parameters

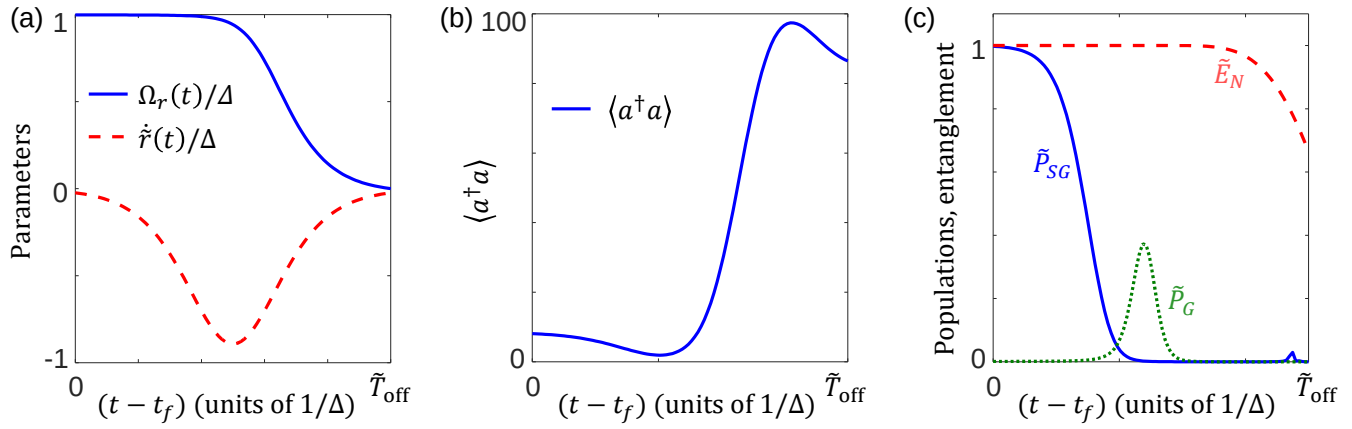

FIG. S4: System evolution during turning off the parametric drive in the adiabatic protocol for $t > t_f$. (a) Amplitude of the parametric drive $\Omega_r(t)$ and the changing rate $\dot{\tilde{r}}(t)$ of the squeezing parameter $r(t)$. (b) Mean photon number $\langle a^\dagger a\rangle$ of the system. (c) Blue-solid curve: the population $\tilde{P}_{SG}$ of the squeezed state $|SG\rangle$; Green-dotted curve: the population $\tilde{P}_G$ of the ground state $|G\rangle$; Red-dashed curve: the entanglement cost (characterized by the logarithmic negativity $\tilde{E}_N$). The time required to turn off the parametric drive is assumed to be $\tilde{T}_{\rm off} = 5/\Delta$.

used in the adiabatic protocol. The parameter $\tilde{*}$ has the same physical meaning as $*$. Due to the squeezing-induced noise, the adiabatic protocol becomes unreliable for the finite cooperativity C [see the blue-dotted curve in Fig. S3(c)].

To minimize the parameters $|\tilde{N}_S|$ and $|\tilde{M}_S|$, we can assume

$$\tilde{r}_e = \begin{cases} 0, & (0 \lesssim t \lesssim \tilde{T}/2) \\ \tilde{r}_{\max}, & (\tilde{T}/2 \lesssim t \lesssim \tilde{T}) \end{cases} \tag{S25}$$

resulting in

$$\tilde{r}_S(t) = \begin{cases} \dfrac{\tilde{r}_{\max}}{1+\exp\left[\tilde{f}_0(1/2-t/\tilde{T})\right]}, & (0 \lesssim t \lesssim \tilde{T}/2) \\ \dfrac{-\tilde{r}_{\max}}{1+\exp\left[-\tilde{f}_0(1/2-t/\tilde{T})\right]}. & (\tilde{T}/2 \lesssim t \lesssim \tilde{T}) \end{cases} \tag{S26}$$

Accordingly, the average values of $|\tilde{N}_S|$ and $|\tilde{M}_S|$ are

$$\tilde{A}_{N_S} = \frac{1}{\tilde{T}}\int_0^{t_f} |\tilde{N}_S| dt \approx 0.14, \quad \text{and} \quad \tilde{A}_{M_S} = \frac{1}{\tilde{T}}\int_0^{t_f} |\tilde{M}_S| dt \approx 0.3, \tag{S27}$$

respectively. Thus, the additional noises characterized by $\tilde{N}_S$ and $\tilde{M}_S$ can be suppressed as shown in Fig. S3(a) and S3(b). The fidelity of the squeezed ground state $|SG\rangle = S(t_f)|G\rangle$ is improved [see the red-solid curve in Fig. S3(c)]. However, due to

$$\tilde{A}_{N_S} > A_{N_S}, \quad \tilde{A}_{M_S} > A_{M_S}, \quad \text{and} \quad \tilde{T} \gg T, \tag{S28}$$

the squeezing-induced noise still affects the adiabatic protocol more seriously than the STA protocol. Thus, the fidelity of the adiabatic protocol is much lower than the STA method, according to the comparison between Figs. S1(c) and S3(c).

S2. A POSSIBLE PROBLEM CAUSED BY TURNING OFF THE PARAMETRIC DRIVE IN THE ADIABATIC PROTOCOL

The nonadiabatic transition $H_{\rm NA}(t)$ also causes the main problem of how to turn off the parametric drive. In the adiabatic protocol discussed in the main text, the amplitude of the parametric drive $\Omega_r(t)$ reaches the peak value at

the time t_f, i.e., $\Omega_r(t_f)=\Omega_{\max}$. Meanwhile, the maximally entangled cat state is prepared in the squeezed frame. In the laboratory frame, the final state corresponds to the qubit being entangled with the squeezed and displaced cavity pointer states, i.e., $|SG\rangle$. To smoothly and rapidly turn off the parametric drive, we can assume

$$\tilde{r}(t)=\frac{1}{2}\frac{\text{arctanh}(\Omega_{\max}/\Delta)}{1+\exp\{10[-(t-t_f)/\tilde{T}_{\text{off}}+1/3]\}},\qquad (t\geq t_f) \tag{S29}$$

corresponding to

$$\tilde{r}(t_f)=\frac{1}{2}\text{arctanh}(\Omega_{\max}/\Delta),\quad \tilde{r}(t_f+\tilde{T}_{\text{off}})\simeq 0,\quad \dot{\tilde{r}}(t_f)\simeq 0,\quad \dot{\tilde{r}}(t_f+\tilde{T}_{\text{off}})\simeq 0. \tag{S30}$$

Here, $\tilde{T}_{\text{off}}$ is the operation time required to turn off the parametric drive.

Assuming $\tilde{T}_{\text{off}}=5/\Delta$ as an example, we show $\Omega_r(t)$ and $\dot{\tilde{r}}(t)$ versus time in Fig. S4(a). Due to $\dot{\tilde{r}}(t)\neq 0$, the nonadiabatic transition $H_{\text{NA}}(t)$ can pump many photons into the cavity. By substituting Eq. (S29) into Eq. (S2), and assuming the system is in the squeezed ground state $|SG\rangle$ at the time t_f, we show the instantaneous mean photon number $\langle a^\dagger a\rangle$ when $t>t_f$ in Fig. S4(b). We find that $\langle a^\dagger a\rangle$ increases sharply when $\Omega_r(t)$ decreases. When the parametric drive is turned off, i.e., $\Omega_r(t)=0$, the desired entangled state does not exist any longer [see in Fig. S4(c)]. Both populations of the squeezed ground state $|SG\rangle$ ($\tilde{P}_{SG}$) and the state $|G\rangle$ ($\tilde{P}_G$) reach 0 when the parametric drive is turned off [see the blue-solid and green-dotted curves in Fig. S4(c)]. The entanglement cost (characterized by the logarithmic negativity $\tilde{E}_N$) decreases to a low value, i.e., $\tilde{E}_N\sim 70\%$. That is, the state of the system after turning off the parametric drive is unpredictable.

[S1] M. O. Scully and M. S. Zubairy, *Quantum Optics* (Cambridge University Press, Cambridge, 1997).